

1 KEYWORDS: Carbon Fiber Reinforced Polymers, Concrete, Steel stirrups, Shear strengthening, Shear failure, Near
2 Surface Mounted (NSM)
3

4 1. INTRODUCTION

5 To increase the shear resistance of concrete beams, sheets and laminates of carbon fiber reinforced polymers
6 (CFRP) are generally applied on the faces of the elements to be strengthened, using an externally bonded reinforcing
7 (EBR) technique. Adopting the EBR technique, several researchers have verified that the shear resistance of
8 concrete beams can significantly be increased¹⁻⁶. However, due to premature debonding of the FRP, the maximum
9 strain mobilized by these systems is well below their ultimate strain.

10 In an attempt to overcome this drawback, a promising strengthening innovation has been proposed by De Lorenzis⁷.

11 Using rods of CFRP embedded into grooves on the concrete cover of lateral faces of the beams, a significant
12 increase on beam load carrying capacity was obtained. Assuring the proper bond conditions for the rod into the
13 groove is the critical phase of this strengthening technique, since it requires special equipment, well-prepared
14 technical staff and a time consuming execution period. In the experimental program carried out by De Lorenzis and
15 Nanni⁸ for the characterization of the bond properties of NSM FRP rods, the grooves were created by saw-cutting
16 two parallel slits at the desired distance and depth, and chiseling off the material in between, which is a time
17 consuming procedure for real applications. In another experimental program⁹, the grooves were pre-formed rather
18 than cut after concrete hardening. This procedure only replicates the real conditions if the concrete cover of the
19 element to be strengthened is deteriorated and needs to be replaced. In such a case, pre-form the grooves while
20 reconstructing the element geometry might be a correct strategy.

21 In the present work, a technique similar to the previous one was used for the shear strengthening of concrete beams
22 with the difference that, instead of rods, laminate strips were used. Since the laminates had a cross section of about
23 $1.4 \times 10 \text{ mm}^2$, they were installed into thin slits, which were easily cut using conventional saw-cut equipments.
24 Furthermore, a high uniformity on the cross section dimensions of the slits can be assured, with the derived benefit
25 of homogeneity in CFRP-concrete bond properties. This strengthening technique has already proven to be very
26 effective for the flexural strengthening of reinforced concrete columns¹⁰ and beams¹¹. The bond behavior was also
27 well characterized by pullout bending tests¹² and a local bond stress-slip relationship was evaluated¹³, which can be
28 used in the analysis and design of concrete elements strengthened by this technique.

29 To evaluate the efficacy of the shear strengthening technique proposed in the present work, the behavior of beams
30 strengthened according to this technique was compared to the behavior of beams reinforced with conventional steel

1 stirrups and with the behavior of beams strengthened by strips of wet lay-up CFRP sheet. The experimental program
2 was designed to analyze the influences of beam depth, NSM laminate strip inclination, and longitudinal tensile steel
3 reinforcement ratio on the shear strengthening. In the present work, the tests carried out are described and the main
4 results are presented and analyzed.

5 The performance of the *ACI*¹⁴ and *fib*¹⁵ analytical formulations for the EBR shear strengthening was appraised.
6 Additionally, the performance of the analytical formulation proposed by Nanni *et al.*¹⁶ is assessed.

8 2. EXPERIMENTAL PROGRAM

9 TEST SERIES

10 The experimental program is composed of four series of tests (Table 1 and Fig. 1). Each series is made up of a beam
11 without any shear reinforcement (C) and a beam for each of the following shear reinforcing systems: steel stirrups of
12 $\phi 6$ mm (S), U shaped strips of CFRP sheet (M) and CFRP laminate strips at 45° (IL) or at 90° (VL) with the beam
13 axis. Series A10 and A12 are composed of beams with a cross section of 0.15×0.30 m² and a span length of 1.5 m.
14 Series B10 and B12 are constituted of beams with a cross section of 0.15×0.15 m² and a span length of 0.9 m. To
15 evaluate the influence of the longitudinal tensile steel reinforcement ratio, ρ_{sl} , series A10 and B10 had $4\phi 10$ steel
16 bars at beam bottom tensile surface, while A12 and B12 series had $4\phi 12$. The shear span, a , (Fig. 1) in both series of
17 beams, was two times the depth of the corresponding beams. At top surface, the beams of all series were reinforced
18 with $2\phi 6$ steel bars. The concrete clear cover for the top, bottom and lateral faces of the beams was 15 mm.

19 The amount of shear reinforcement applied on the four reinforcing systems was designed such that all beams would
20 fail in shear, at a similar maximum load. For this purpose, the strategy adopted on the evaluation of the distinct shear
21 reinforcing systems was the following. The beam flexural load carrying capacity, $F_{rupture}^{flexural}$, for each ρ_{sl} was
22 evaluated. The concrete contribution for the beam shear resistance was determined according to the Portuguese
23 Code, that is similar to the CEB-FIP Model Code¹⁷ but the dowel effect is not considered ($V_{cd}^{ana} = \tau_1 b_w d$, where τ_1
24 is the concrete shear strength and b_w and d are the beam width and the effective depth, respectively). The percentage
25 of steel stirrups was evaluated according to Portuguese Code ($V_{wd}^{ana} = 0.9d \frac{A_{sw}}{s} f_{syd}$, where s , f_{syd} and A_{sw} are the
26 spacing, the design yield stress and the cross section area of the two arms steel stirrups, respectively). This
27 percentage was determined in order to provide a beam shear load carrying capacity ($2 V_{cd}^{ana} + 2 V_{wd}^{ana}$) lesser than

1 $F_{rupture}^{flexural}$. According to the arrangements of the steel stirrups adopted in the beam series (Fig. 1), the
2 $F_{rupture}^{flexural} / (2V_{cd}^{ana} + 2V_{wd}^{ana})$ ratio was 1.05, 1.08, 1.5 and 1.37 for the A10, A12, B10 and B12 series.
3 The percentage of the CFRP shear reinforcing systems was evaluated to provide a contribution for the beam shear
4 resistance similar to the one of the steel stirrups. For the strips of wet lay-up CFRP sheets of U shape, the
5 recommendations of the ACI Committee 440 were followed¹⁴. For the NSM CFRP laminate strips, the formulation
6 used for the steel stirrups was adopted, but the yield stress was replaced by an effective stress that was determined
7 assuming a CFRP strain value of 4‰, that is the maximum effective strain value recommended by ACI Committee
8 440 for the EBR shear reinforcing systems.
9 Steel stirrups were not applied in the series reinforced with CFRP systems. The interaction between the CFRP shear
10 reinforcement and the steel stirrups will be only investigated in future experimental programs.

11

12 *MATERIAL PROPERTIES*

13 *Concrete and steel bars*

14 The average compression strength (f_{cm}) at 28 days and at the date of beam testing was evaluated from uniaxial
15 compression tests with cylinders of 150 mm diameter and 300 mm height. At 28 days, series A and B had a f_{cm} of
16 37.6 and 49.5 MPa, respectively. At beam testing age of 227 and 105 days for series A and B, respectively, the f_{cm} of
17 series A and B was 49.2 and 56.2 MPa. The properties of the steel bars were obtained from uniaxial tensile tests,
18 carried out according to European standard EN 10 002-1¹⁸. The registered results are included in Table 2.

19

20 *CFRP systems*

21 Unidirectional wet lay-up sheets of a trademark S&P C-Sheet 530 and precured laminates of a trademark S&P
22 laminate CFK 150/2000 were the two CFRP systems used in the present work. According to the supplier, tensile
23 strength (f_{fu}^*), Young's modulus (E_f) and ultimate strain (ε_{fu}^*) of the sheets and laminates have the following values:
24 $f_{fu}^* = 3000$ MPa, $E_f = 390000$ MPa and $\varepsilon_{fu}^* = 0.8\%$ for sheets; and $f_{fu}^* = 2200$ MPa, $E_f = 150000$ MPa and $\varepsilon_{fu}^* = 1.4\%$
25 for laminates. The sheet had a thickness of 0.167 mm, while the cross section of the S&P laminate CFK 150/2000
26 had a width of 10 mm and a thickness of 1.4 mm. For the laminates, six tests were also carried out according to the
27 ISO 527-5 recommendations¹⁹, from which the following average values were obtained: $f_{fu} = 2286$ MPa,
28 $E_f = 166000$ MPa and $\varepsilon_{fu} = 1.3\%$.

29

1 *STRENGTHENING TECHNIQUES*

2 The EBR and NSM strengthening techniques are represented in Fig. 2. To apply the wet lay-up CFRP strengthening
3 system, the following procedures were done: 1) on the zones of the beam's surfaces where the strips of CFRP sheet
4 would be glued, an emery was applied to remove the superficial cement paste and to round out the beam edges; 2)
5 the residues were removed by compressed air; 3) a layer of primer was applied to regularize the concrete surface and
6 to enhance the adherence capacity of the concrete substrate; and 4) strips of U shape CFRP sheet, composed of two
7 layers, were glued to the bottom and to the lateral faces of the beam, by epoxy resin.

8 To apply the precured laminate strips, the following procedures were mobilized: 1) slits of about 5 mm width and
9 12 mm depth were made, in previously marked places, on both lateral surfaces of the beam; 2) the slits were cleaned
10 by compressed air; 3) the laminates were cleaned by acetone; 4) the slits were filled with epoxy adhesive
11 manufactured according to the supplier recommendations; 5) a thin layer of epoxy adhesive was applied on the faces
12 of the CFRP laminates; and 6) the CFRP laminates were introduced into the slits after which the excess epoxy
13 adhesive was removed.

14

15 *TEST SET-UP*

16 The beams were subjected to four point loads (Fig. 1). The force was measured from a load cell of 300 kN
17 maximum capacity and 0.06 % linearity. To evaluate the beam deflection, five LVDTs of 25 mm and 50 mm full
18 stroke were used, placed at mid span, under point loads and at middle of the shear span. To avoid the register of
19 extraneous deflections (concrete crushing at beam supports, deformability of the reaction frame, etc), the LVDTs
20 were supported on a "Japanese Yoke" system²⁰. The tests were carried out under displacement control, using a
21 deflection rate of 10 $\mu\text{m/s}$ imposed on the LVDT placed at the beam mid span.

22

23

23 **3. RESULTS**

24

25 Defining F_{max,K_C} and F_{max,K_S} as the maximum load of a beam without shear reinforcement and a beam reinforced
26 with steel stirrups, respectively, (K represents the series of tests) the ratios $F_{max,K}/F_{max,K_C}$ and $F_{max,K}/F_{max,K_S}$ were
27 determined to assess the efficacy of the shear strengthening techniques, in terms of the increase of the beam load
28 carrying capacity. To define the deformation capacity and the retention of the load carrying capacity in the structural
29 softening phase of the beams, provided by each shear strengthening technique, a deflection, $\delta_{p,K}$, corresponding to
30 $0.95F_{max,K}$, beyond the deflection at the peak load, $\delta_{F_{max,K}}$, was determined (Fig. 3). This deflection level was

1 selected since it represents the beam deformation capacity for a reduced loss of the beam load carrying capacity
2 (only 5%) in the structural softening phase. The deformation capacity was evaluated from the ratios $\delta_{p,K}/\delta_{p,K_C}$ and
3 $\delta_{p,K}/\delta_{p,K_S}$ (termed the deformability indices) where δ_{p,K_C} and δ_{p,K_S} are the deflections for $0.95F_{max,K_C}$ and
4 $0.95F_{max,K_S}$, respectively.

6 *A10 SERIES*

7 For the A10 series, the relationship between the force and the deflection at beam mid span is depicted in Fig. 4.
8 Table 3 includes the main results obtained in this series. When compared to the maximum force of the unreinforced
9 beam (A10_C), Fig. 4 and Table 3 show that the CFRP shear strengthening systems increased the maximum load
10 between 22% (A10_M) and 58% (A10_VL and A10_IL). The F_{max} of the A10_M, A10_VL and A10_IL beams
11 (strengthened with CFRP systems) was 28%, 6% and 7% less than the F_{max} of the beam reinforced with steel stirrups
12 (A10_S). The highest deformation capacity was registered in the beam strengthened with inclined laminates
13 (A10_IL). In comparison with $\delta_{p,A10_C}$ (unreinforced beam), the $\delta_{p,A10_S}$, $\delta_{p,A10_M}$, $\delta_{p,A10_VL}$ and $\delta_{p,A10_IL}$ were 480%,
14 34%, 359% and 1006% larger. When compared to the beam reinforced with steel stirrups (A10_S), the deformation
15 capacity of the A10_IL beam was 91% higher.

17 *A12 SERIES*

18 Fig. 5 depicts, for the A12 series, the relationship between the force and the deflection at beam mid span. Table 3
19 includes the main results obtained in this series. Taking the F_{max} of A12_C beam as a reference value, the steel
20 stirrups provided an 85% increase in F_{max} , while CFRP strengthening systems assured an increase ranging between
21 54% and 125%, having highest one been registered in the beam strengthened with inclined laminates (A12_IL), and
22 the lowest one in the beam with strips of wet lay-up sheet (A12_M). Comparing the F_{max} of the beams strengthened
23 by CFRP systems with the beam reinforced with steel stirrups (A12_S), the F_{max} of A12_M, A12_VL and A12_IL
24 beams was 17% smaller, 9% and 22% larger, respectively. The higher efficacy of the laminates at 45° was also
25 notable in terms of deformation capacity. When compared with δ_p of beam A12_C ($\delta_{p,VA12_C}$), the δ_p of A12_S,
26 A12_VL and A12_IL beams was 131%, 145% and 329% larger, respectively, i.e., the beam strengthened with
27 inclined laminates had an 85% higher deformation capacity than the beam reinforced with steel stirrups. The
28 deformation capacity of the A12_M beam was 77% of the A12_S beam.

1 *B10 SERIES*

2 For the B10 series, Fig. 6 illustrates the relationship between the force and the deflection at beam mid span. The
3 main results are included in Table 3. Taking into account the load of the beam without any shear reinforcement,
4 $F_{max,B10_C}$, the steel stirrups provided a 63% increase on the F_{max} , while the increase assured by CFRP shear
5 strengthening systems ranged between 50% and 77%, having highest one been registered in the beam with vertical
6 laminates (B10_VL), and the lowest one in the beam with strips of sheet (B10_M). Taking the maximum force of
7 the beam reinforced with steel stirrups ($F_{max,B10_S}$) as a basis of comparison, it was verified that the maximum load of
8 B10_M, B10_VL and B10_IL beams was 92%, 109% and 100% of the $F_{max,B10_S}$, respectively. The better
9 performance of the vertical laminate shear reinforcing system was more pronounced in terms of beam deformation
10 capacity. In fact, the beams reinforced with steel stirrups, vertical laminates, inclined laminates and strips of sheet
11 had a δ_p 327%, 242%, 114% and 120% larger than the δ_p of the beam without any shear reinforcement. The
12 deformation capacity of the beam reinforced with vertical laminates was 80% of the beam reinforced with steel
13 stirrups.

14

15 *B12 SERIES*

16 For the B12 series, the relationship between the force and the deflection at beam mid span is depicted in Fig. 7. The
17 main results are included in Table 3. When compared to the maximum load of the beam without any shear
18 reinforcement, $F_{max,B12_C}$, it is observed that steel stirrups provided an increase of 110% in the F_{max} , while the
19 increase assured by CFRP shear strengthening systems ranged from 84% to 96%, having the highest one been
20 recorded in the beam with inclined laminates (B12_IL), and the lowest one in the beam with vertical laminates
21 (B12_VL). Using the maximum force of the beam reinforced with steel stirrups ($F_{max,B12_S}$) as a basis of comparison,
22 it was verified that the maximum load of B12_M, B12_VL and B12_IL beams was 90%, 87% and 93% of the
23 $F_{max,B12_S}$, respectively. In terms of deformation capacity, the better CFRP strengthening system was the one
24 composed of inclined laminates. When the δ_p of the beam without any shear reinforcement ($\delta_{p,B12_C}$) is compared to
25 the δ_p of the remaining beams, an increase of 151%, 73%, 119% and 142% was obtained in the B12_S, B12_M,
26 B12_VL and B12_IL beams, respectively, showing that the deformation capacity of the beam with inclined
27 laminates was 97% of the beam reinforced with steel stirrups.

28

29

30

1 FAILURE MODES

2 Figs. 8 to 11 include photos of the beams after they have been tested. A representation of the failure modes is also
3 depicted. The unreinforced shear C beams have failed by the formation of one shear failure crack without the
4 yielding of the longitudinal tensile reinforcement. A shear failure crack occurred in the beams reinforced with steel
5 stirrups (S beams). However, in beams A10_S (Fig. 8) and A12_S (Fig. 9) this shear failure crack occurred after the
6 yielding of the longitudinal tensile reinforcement since the flexural load carrying capacity ($F_{rupture}^{flexural}$) of these beams
7 is only 5% to 8% higher than the combined contribution of the concrete and steel stirrups ($2 V_{cd}^{ana} + 2 V_{wd}^{ana}$) for the
8 beam shear resistance (see subsection “Test Series” of Section 2). Since $F_{rupture}^{flexural}$ of the beams B10_S (Fig. 10) and
9 B12_S (Fig. 11) is 50% and 37% higher than the $2 (V_{cd}^{ana} + V_{wd}^{ana})$ of these beams, they were failed by the formation of
10 a shear crack before the yielding of the longitudinal tensile reinforcement.

11 The sudden loss of the load carrying capacity in the S beams corresponds to the moment when a steel stirrup,
12 crossing the shear failure crack, ruptured. Due to the combined crack opening and crack sliding of the shear failure
13 crack, a stress gradient occurred in the cross section of the steel stirrup crossing the shear failure crack, leading to its
14 rupture. This stress gradient was significant since only one steel stirrup was bridging the shear failure crack.

15 In general, beams M failed by the formation of a shear crack. In Figs. 8 to 11, the darkest parts of the CFRP strips
16 represent the length that peeled-off. Due to the U configuration of the CFRP strips, the peeled-off process
17 propagated from the top to the bottom of the beam (Fig. 12a). In these beams, immediately after the CFRP strips
18 crossing the shear failure crack have peeled-off, the CFRP strips crossing the horizontal path of the shear crack have
19 ruptured due to an abrupt increment of tensile and shear stresses in the CFRP, as a result of the crack opening and
20 crack sliding (Fig. 12a). B12_M beam (Fig. 12b) had a distinct failure mode. This beam has failed by the formation
21 of two “concrete lateral walls” that have separated from the interior concrete volume. A shear crack formed in this
22 interior concrete volume and, finally, the “lateral walls” ruptured. The justification for this distinct failure mode can
23 reside on the ratio between the area of the CFRP strips bonded to the beam lateral surfaces and the area of the beam
24 lateral surfaces, since it is the highest one of the M beams. Due to the high percentage of CFRP strips of beam
25 B12_M, the shear failure crack did not extend to the total width of the beam. Two lateral walls of 15 to 20 mm thick,
26 reinforced with the strips, have spoiled, resulting a failure mode composed by the beam core, failed in shear, and
27 two lateral reinforced walls, detached from this core.

28 This complex type of failure also occurred in beams B10_IL, B12_VL and B12_IL, due to similar reasons (Fig.
29 12c).

1 In A10_VL beam, after the yielding of the longitudinal tensile reinforcement, a shear failure crack formed. During
2 the opening process of this crack, the shorter bond length of the CFRP laminate strip crossing this crack slip (Fig.
3 12d).

4 Beams A12_VL failed in shear and the shorter bond length of the CFRP laminate strip crossing this crack slip.
5 Finally, beams A10_IL and A12_IL ruptured by the formation of a flexural failure crack.

6
7 *INFLUENCE OF TEST PARAMETERS ON THE EFFICACY OF THE CFRP SHEAR STRENGTHENING*
8 *SYSTEMS*

9 Fig. 13 represents the influence of the CFRP shear reinforcement ratio (ρ_f), the beam depth (h) and the longitudinal
10 tensile steel reinforcement (ρ_{sl}) on the beam load carrying capacity provided by the considered CFRP shear
11 reinforcing systems. The ΔF_{max} corresponds a two times the contribution of the CFRP systems for the beam shear
12 resistance (V_f), since $\Delta F_{max} = F_{max,K} - F_{max,K_C} = 2 V_f$. To take into account the distinct values of the Young's modulus
13 of the CFRP materials, the ρ_f of the CFRP sheets was converted into an equivalent percentage of CFRP laminates,
14 multiplying its percentage by the E_{f_M}/E_{f_L} parameter, where E_{f_M} and E_{f_L} are the Young's modulus of the sheets and
15 laminates, respectively.

16 From the analysis of Fig. 13a it can be concluded that ΔF_{max} increased with ρ_f and this increase was most
17 significant in the highest beams strengthened by NSM technique. Fig. 13b shows that, for the beams strengthened by
18 EBR technique the ΔF_{max} decreased with the increase of the beam depth, while in the beams strengthened by NSM
19 technique the ΔF_{max} increased with the increase of the beam depth. This increase was more pronounced in the beams
20 of high longitudinal tensile reinforcement ratio ($4\phi 12$), mainly when laminates are positioned at 45-degrees. This
21 can be justified by the values of the total effective length of the CFRP laminates ($L_{tot\ min}$) contributing for the beam
22 shear resistance, which concept is described in Subsection “*FORMULATION BY NANNI ET AL. FOR NSM*
23 *TECHNIQUE*” of Section 4, since it was verified that ΔF_{max} has an increase linear trend with $L_{tot\ min}$, and the
24 maximum $L_{tot\ min}$ corresponds to A12_IL beam (see, for a while, Fig. 20).

25 Fig. 13c reveals that ΔF_{max} increased with ρ_{sl} and this increase was more pronounced in the highest beams
26 strengthened by the NSM technique.

27

28

1 PROFITABILITY OF THE NSM TECHNIQUE

2 To assess the influence of the CFRP laminate orientation, not only in terms of increasing the beam load carrying
3 capacity (F_{max}), but also in terms of the amount of consumed CFRP, the ratio $\Delta F_{max}/l_{CFRP}$ of the beams strengthened
4 by the NSM technique was evaluated (designated by profitability index), where ΔF_{max} is the increase in the F_{max} and
5 l_{CFRP} is the total length of the laminates applied in the beam. The values included in Table 4 show that (see also Fig.
6 14), independent of the beam height and the longitudinal steel reinforcement ratio (ρ_{sl}), the profitability index was
7 larger in the beams with laminates at 45°. For both the A series, the profitability index increased with the increase of
8 ρ_{sl} . This tendency was not observed in both B series since the reduced bonded lengths of the CFRP laminates in
9 these shallow beams limited the increase on the ΔF_{max} .

10

11

4. APPRAISAL THE PERFORMANCE OF ANALYTICAL FORMULATIONS

12 Taking the results obtained in the tested beams strengthened with EBR technique, the performance of the analytical
13 formulations proposed by *ACI*¹⁴ and *fib*¹⁵ was appraised. The documents published by these institutions are not yet
14 dealing with the NSM technique. Thereby, the applicability of the analytical formulation proposed by Nanni *et al.*¹⁶
15 was checked, using for this purpose the experimental results obtained in the beams strengthened with NSM
16 laminates. New estimates for the parameters of the model by Nanni *et al.* are proposed in order to take into account
17 the bond stress and the CFRP effective strain values recorded in pullout bending tests¹².

18

19 ACI RECOMMENDATIONS FOR EBR TECHNIQUE

20 According to *ACI*¹⁴, the design value of the contribution of the FRP shear reinforcement is given by,

$$V_{fd} = \phi \psi_f \frac{A_{fv} f_{fe} d_f}{s_f} \quad (1)$$

21 where ϕ is the strength-reduction factor required by *ACI*²¹ that, for shear strengthening of concrete elements, has a
22 value of 0.85, ψ_f is an additional reduction factor of 0.85 for the case of three-sided U-wraps (see Fig. 15), s_f is the
23 spacing of the wet lay-up strips of FRP sheets, A_{fv} is the area of FRP shear reinforcement within spacing s_f ,

$$A_{fv} = 2 n t_f w_f \quad (2)$$

24 with n , t_f and w_f being the number of layers per strip, the thickness of a layer and the width of the strips. The
25 effective stress in the FRP, f_{fe} , is obtained multiplying the Young's modulus of the FRP, E_f , by the effective strain,

$$\varepsilon_{fe} = k_v \varepsilon_{fu} \leq 0.004 \quad (\text{for U-wraps}) \quad (3)$$

1 where k_v is a bond-reduction coefficient that is a function of the concrete strength, the type of wrapping scheme
 2 used, and the stiffness of the FRP,

$$k_v = \frac{k_1 k_2 L_e}{11900 \varepsilon_{fu}} \leq 0.75 \quad (4)$$

3 with,

$$L_e = \frac{23300}{(n t_f E_f)^{0.58}} \quad (5)$$

$$k_1 = \left(\frac{f'_c}{27} \right)^{2/3} \quad (6)$$

$$k_2 = \frac{d_f - L_e}{d_f} \quad (\text{for U-wraps}) \quad (7)$$

4 In (1) and (7) d_f is the depth of FRP shear reinforcement (see Fig. 15), and f'_c is the characteristic value of the
 5 concrete compression strength²¹. The length and the force unities of the variables in (4) to (7) are millimeter and
 6 Newton, respectively.

7 In Table 5, the values obtained with this formulation are compared to those registered experimentally. Apart beam
 8 B10_M, the *ACI* formulation has estimated a FRP contribution for the shear strengthening that was larger than the
 9 contribution recorded experimentally. A deficient bond of the strip crossed by the shear failure crack might have
 10 caused the high abnormal value of $V_{fd}^{ana.} / V_f^{exp.}$ of A10_M beam, since this strip has debonded prematurely (see
 11 Fig. 8).

12
 13 *fib RECOMMENDATIONS FOR EBR TECHNIQUE*

14 According to *fib* recommendations¹⁵, the contribution of wet lay-up strips of FRP sheets for shear strengthening is
 15 evaluated by the following expression,

$$V_{fd} = 0.9 \varepsilon_{fe,d} E_f \rho_f b_w d \quad (8)$$

16 where b_w and d are the width of the beam cross section and the distance from extreme compression fiber to the
 17 centroid of the nonprestressed steel tension reinforcement. In (8) ρ_f is the FRP shear reinforcement ratio,

$$\rho_f = \frac{A_{fv}}{b_w s_f} \quad (9)$$

1 and $\varepsilon_{fe,d}$ is the design effective strain in the FRP, that can be obtained from ε_{fe} ,

$$\varepsilon_{fe} = \min \left[0.65 \left(\frac{f_{cm}^{2/3}}{E_f \rho_f} \right)^{0.56} \times 10^{-3}; 0.17 \left(\frac{f_{cm}^{2/3}}{E_f \rho_f} \right)^{0.30} \varepsilon_{fu} \right] \quad (f_{cm} \text{ in MPa and } E_f \text{ in GPa}) \quad (10)$$

2 applying two safety factors, $\varepsilon_{fe,d} = 0.8\varepsilon_{fe}/1.3$, the first one, 0.8, to convert ε_{fe} in a characteristic value and the
3 second one, 1.3, that depends on the FRP failure mode (in the present case the beams strengthened with EBR
4 technique failed by debonding). In (10) f_{cm} is the cylinder average concrete compression strength and ε_{fu} is the
5 ultimate FRP strain. The analytical and the experimental results are compared in Table 5. Apart beam B12_M, *fib*
6 formulation has also predicted an FRP contribution larger than the experimentally registered values. Like in the *ACI*
7 formulation, an abnormal high $V_{fd}^{ana.} / V_f^{exp.}$ value was also obtained in A10_M beam, which stresses the suspicious
8 that the strip crossing the shear failure crack was deficiently bonded.

9
10 Fig. 16 compares the values of the CFRP contribution for the shear strengthening according to *ACI* and *fib*
11 formulations. In general, all the formulations estimated larger values than the ones registered experimentally. Apart
12 B12_M beam, in the remaining beams the *ACI* formulation estimated lower values than *fib*.

13 Using similar EBR shear strengthening configuration, other researchers have obtained larger safety factors.
14 However, these researchers have used wet lay-up CFRP sheets of Young's modulus (E_f) of about 220 GPa, and, in
15 the major cases, the shear CFRP strips were formed of one layer. In the present research a CFRP sheet of
16 $E_f=390$ GPa and strips of two layers were used. This indicates that the expressions of *ACI* and *fib* formulations
17 defining the FRP effective strain were not well calibrated for this situation, since they are providing too high
18 effective strain values when using stiffer shear CFRP systems. Therefore, more research is needed in this field.

19

20 FORMULATION BY NANNI ET AL. FOR NSM TECHNIQUE

21 According to the formulation by Nanni *et al.*¹⁶, the contribution of the NSM FRP elements for the shear
22 strengthening is obtained from expression,

$$V_f = 4 \cdot (a_f + b_f) \cdot \tau_b \cdot L_{tot \min} \quad (11)$$

23 where a_f and b_f are the dimensions of the laminate cross section, τ_b represents the average bond stress of the FRP
24 elements intercepted by the shear failure crack, and $L_{tot \min}$ is obtained from (see Fig. 17),

$$L_{tot\ min} = \sum_i L_i \quad (12)$$

1 where L_i represents the length of each single NSM laminate intercepted by a 45-degree shear crack expressed as,

$$L_i = \begin{cases} \min\left(\frac{s_f}{\cos \alpha + \sin \alpha} i; l_{max}\right) & i = 1, \dots, \frac{N}{2} \\ \min\left(l_{net} - \frac{s_f}{\cos \alpha + \sin \alpha} i; l_{max}\right) & i = \frac{N}{2} + 1, \dots, N \end{cases} \quad (13)$$

2 $L_{tot\ min}$ corresponds to an arrangement of the FRP reinforcements crossing the shear failure crack that leads to the
3 minimum of the $\sum_i L_i$. In (13) α represents the slope of the FRP laminate with respect to the beam longitudinal axis

4 and l_{net} is defined as,

$$l_{net} = l_b - \frac{2c}{\sin \alpha} \quad (14)$$

5 which represents the net length of a FRP laminate, as shown in Fig. 17, to account for cracking of the concrete cover
6 and installation tolerances. In (14), l_b is the actual length of a FRP laminate and c is the concrete clear cover.

7 The first limitation of (13) takes into account bond as the controlling failure mechanism, and represents the
8 minimum effective length of a FRP laminate intercepted by a shear crack as a function of the term N :

$$N = \frac{l_{eff} (1 + \cot \alpha)}{s_f} \quad (15)$$

9 where N is rounded off to the lowest integer (e.g., $N=5.7 \Rightarrow N=5$), and l_{eff} represents the vertical length of l_{net} as
10 shown in Fig. 17 written as follows:

$$l_{eff} = l_b \sin \alpha - 2c \quad (16)$$

11 The second limitation in (13), $L_i = l_{max}$, results from the force equilibrium condition, taking an upper bound value
12 for the effective strain, ε_{fe} (see Fig. 18),

$$l_{max} = \frac{\varepsilon_{fe}}{2} \cdot \frac{a_f \cdot b_f}{a_f + b_f} \cdot \frac{E_f}{\tau_b} \quad (17)$$

13
14 Adopting for ε_{fe} and τ_b the values recommended by Nanni *et al.*¹⁶, 4‰ and 6.9 MPa, respectively, and assuming
15 for the Young's modulus of the laminate the average value recorded in the experimental program of the present
16 work (166 GPa), the values of the contribution of the NSM laminates for the shear strengthening of concrete beams,

1 included in Table 6, are compared to those registered experimentally (for ϕ and ψ_f a value of 0.85 was considered,
2 following the recommendations of ACI ¹⁴). This table does not include the data of the B10_VL beam since,
3 according to the formulation by Nanni *et al.*, the FRP contribution is null. An average $V_f^{exp.}/V_{fd}^{ana.}$ ratio of about
4 2.51 was obtained, which is significantly larger than the value determined by Nanni *et al.* ¹⁶, which indicates that for
5 τ_b and/or ε_{fe} a too conservative values were adopted.

6 Since the value of 6.9 MPa for the τ_b was obtained from bond tests with round cross sectional FRP bars, pullout-
7 bending tests ¹², schematically represented in Fig. 19, were carried out to assess the average bond stress for the used
8 rectangular cross sectional CFRP laminates. The specimen was composed of two blocks: block B where the CFRP
9 was fixed to concrete along a bonded length of 325 mm; block A where the CFRP was bonded to concrete using
10 distinct bond lengths (test region). This configuration assured that the bond failure would occur in block A. The slit
11 where the CFRP was inserted had a 15 mm depth and a 3.3 mm width. The displacement transducer LVDT2 was
12 used to control the test, at 5 $\mu\text{m/s}$, and to measure the slip at the loaded end, u_l , while LVDT1 recorded the slip at
13 the free end, u_f . The strain gauge glued to the CFRP at the symmetry axis of the specimen was used to estimate the
14 pullout force on the CFRP at the loaded end. The applied forces were measured using two load cells (LC1 and LC2)
15 placed at the supports of the specimen. Bond lengths, L_b , of 40, 60 and 80 mm were considered for assessing its
16 influence on bond behavior.

17 From the obtained peak pullout forces a τ_b of 16.1 MPa was determined, which is much larger than the value
18 obtained by De Lorenzis ⁷ for the NSM FRP rod strengthening system ($\tau_b=6.9$ MPa), and recommended by Nanni
19 *et al.* ¹⁶. This difference can be justified by the fact that in the present work the adhesive system in the slit is
20 composed by two thin layers of quasi constant thickness, while in the groove of De Lorenzis ⁷ bond tests the
21 adhesive material had a variable thickness, in consequence of the rectangular geometry of the groove and the
22 circular geometry of the rod cross section.

23 The CFRP average strain (ε_f) in the bond length of the carried out pullout bending tests ¹² was evaluated from the
24 u_l and u_f slips. At peak pullout force, the ε_f of the series of L_b equal to 40, 60 and 80 mm was 4.2‰, 5.7‰ and
25 7.9‰, respectively, giving an average strain of 5.9‰.

26 Assuming that τ_b , ε_f and E_f are equal to 16.1 MPa, 5.9‰ and 166 GPa, respectively, the analytical results
27 indicated in Table 6 were obtained. If the experimental results ($V_f^{exp.}$) are compared to the analytical ones ($V_{fd}^{ana.}$),
28 an average $V_f^{exp.}/V_{fd}^{ana.}$ ratio of about 1.39 was obtained. Since a safety factor of 1.79 ($V_c^{exp.}/V_{cd}^{ana.} = 1.79$) was

1 obtained in the beams without any shear reinforcement (see Table 7), and a safety factor of 1.24 ($V_{sw}^{exp.} / V_{swd}^{ana.} =$
2 1.24) was determined for the contribution of the steel stirrups for the shear resistance, the safety factor of 1.39
3 indicates that the formulation by Nanni *et al.* can be considered for the evaluation of the NSM CFRP laminates in
4 the shear strengthening of concrete beams.

5
6 Expression (11) indicates that V_f is proportional to $L_{tot\ min}$. To check this assumption, Fig. 20 represents the
7 relationship between the ΔF_{max} (equal to two times the contribution of the CFRP systems for the beam shear
8 resistance, V_f) obtained experimentally in the beams strengthened by NSM technique and the $L_{tot\ min}$. From this
9 figure a clear linear increase trend between these two parameters is observed, which the validity of the
10 aforementioned assumption.

11 12 5. CONCLUSIONS

13 To assess the effectiveness of a near surface mounted (NSM) technique for the shear strengthening of concrete
14 beams, four beam series of distinct depth and longitudinal tensile steel reinforcement ratio were tested under four
15 point loads. Each series was composed of one beam without any shear reinforcement and one beam using the
16 following shear reinforcing systems: conventional steel stirrups; strips of wet lay-up CFRP sheet embracing the
17 bottom (in tension) and the lateral beam faces, designated by externally bonded reinforcing (EBR) technique; and
18 laminate strips of CFRP embedded into vertical or inclined (45 degrees) pre-cut slits on the concrete cover of the
19 beam lateral faces (NSM strengthening technique). From the results obtained, the following main conclusions can be
20 pointed out:

- 21 • The load carrying capacity of reinforced concrete beams failing in shear can be significantly increased using
22 the CFRP shear strengthening systems applied in the present work;
- 23 • The NSM shear strengthening technique was the most effective of the CFRP systems. This efficacy was not
24 only in terms of the beam load carrying capacity, but also in terms of deformation capacity at beam failure.
25 Using the load carrying capacity, F_{max} , of the unreinforced beams, for comparison purposes, the beams
26 strengthened by EBR and NSM techniques showed an average increase of 54% and 83%, respectively. The
27 same comparison for the deflection at $0.95F_{max}$ after peak load (designated by deformability index, δ_p), showed
28 that the increments were 77% and 307%, respectively, indicating that the efficacy of the NSM was more
29 pronounced in terms of deformability index;

- 1 • In terms of the F_{max} and the δ_p of the beams reinforced with steel stirrups, the NSM strengthening technique
2 provided almost similar F_{max} and an increase of 9% in the δ_p ;
- 3 • Failure modes of the beams strengthened by the NSM technique were not as brittle as the ones observed in the
4 beams strengthened by the EBR technique;
- 5 • The NSM shear strengthening technique was easier and faster to apply than the EBR technique;
- 6 • The design values of the contribution of the CFRP EBR strengthening systems for the beam shear resistance,
7 evaluated from the *ACI* and *fib* formulations were 2% and 8% higher than the values registered experimentally,
8 respectively;
- 9 • Assuming a bond stress of 16.1 MPa and an effective strain of 5.9‰ (average values of the data recorded in
10 pullout bending tests), the formulation by Nanni *et al.* for the NSM technique predicted a CFRP contribution
11 around 72% of the experimentally registered values, which indicate to be a formulation that can be considered
12 for the design of the contribution of the CFRP NSM shear strengthening system.

14 ACKNOWLEDGEMENTS

15 The authors wish to acknowledge the supports provided by the S&P[®], BeTTor MBT[®] Portugal, Secil (Unibetão),
16 and the colaboration of Cemacom. The study reported in this paper forms a part of the research program
17 “CUTINSHEAR - Performance assessment of an innovative structural FRP strengthening technique using an
18 integrated system based on optical fiber sensors” supported by FCT, POCTI/ECM/59033/2004.

20 REFERENCES

- 21 1. Taerwe, L., Khalil, H. and Matthys S., “*Behaviour of RC beams strengthened in shear by external CFRP*
22 *sheets*”, Proceedings of the Third International Symposium Non-Metallic (FRP) Reinforcement for Concrete
23 Structures, Vol.1, Tokyo, October, 1997, pp. 483-490.
- 24 2. Chaallal, O., Nollet, M.J. and Perraton D., “*Shear strengthening of RC beams by externally bonded side CFRP*
25 *Strips*”, Journal of Composites for Construction, Vol. 2, N° 2, May, 1998, pp. 111-113.
- 26 3. Triantafillou T., “*Shear strengthening of reinforced concrete beams using epoxy-bonded FRP composites*”, ACI
27 Structural Journal, March-April, 1998, pp. 107-115.
- 28 4. Khalifa A., Gold, W.J., Nanni, A. and Aziz M.I.A., “*Contribution of externally bonded FRP to shear capacity of*
29 *RC flexural members*”, Journal of Composites for Construction, Vol. 2, N° 4, November, 1998, pp. 195-202.

- 1 5. Triantafillou T. and Antonopoulos C. P., "*Design of concrete flexural members strengthened in shear with*
2 *FRP*", Journal of Composites for Construction, Vol. 4, N° 4, November, 2000, pp. 198-205.
- 3 6. Basler, M., White, D. e Desroches, M., "*Shear strengthening with bonded CFRP L-shaped plates*", Field
4 Applications of FRP Reinforcement: Case Studies, ACI International SP-215, Editors: Sami Rizkalla and
5 Antonio Nanni, 2003, pp. 373-384.
- 6 7. De Lorenzis, Laura, "*Strengthening of RC Structures with Near-Surface Mounted FRP rods*", PhD Thesis in
7 Civil Engineering, Universita' Degli Studi di Lecce, Italy, May, 2002, 289 pp.
- 8 8. De Lorenzis, L. and Nanni A., "*Characterization of FRP rods as near-surface mounted reinforcement*", Journal
9 of Composites for Construction, Vol. 5, N° 2, May, 2001, pp. 114-121.
- 10 9. De Lorenzis, L., Rizzo. A. and A. La Tegola, "*A modified pull-out test for bond of near-surface mounted FRP*
11 *rods in concrete*", Composites: Part B, N° 33, 2002, pp. 589-603.
- 12 10. Barros, J.A.O., Sena-Cruz, J.M., Dias, S.J.E., Ferreira, D.R.S.M., and Fortes, A.S., "*Near surface mounted*
13 *CFRP-based technique for the strengthening of concrete structures*" Workshop on R+D+I in Technology of
14 *Concrete Structures - tribute to Dr. Ravindra Gettu*, Barcelona, Spain, 2004, pp. 205-217.
- 15 11. Barros, J.A.O., Fortes, A.S., "*Flexural strengthening of concrete beams with CFRP laminates bonded into slits*",
16 Journal of Cement and Concrete Composites, Vol.27, N°4, 2005, pp. 471-480.
- 17 12. Sena-Cruz, J.M. and Barros, J.A.O., "*Bond between near-surface mounted CFRP laminate strips and concrete*
18 *in structural strengthening*", Journal of Composites for Construction, Vol. 8, N° 6, 2004, pp. 519-527.
- 19 13. Sena-Cruz, J.M. and Barros, J.A.O., "*Modeling of bond between near-surface mounted CFRP laminate strips*
20 *and concrete*", Computers and Structures Journal, Vol. 82/17-19, 2004, pp. 1513-1521.
- 21 14. ACI Committee 440, "*Guide for the design and construction of externally bonded FRP systems for*
22 *strengthening concrete structures*", American Concrete Institute, ACI Committee 440, 2002, 118 pp.
- 23 15. fib - Bulletin 14, 2001, "*Externally bonded FRP reinforcement for RC structures*", technical report by Task
24 Group 9.3 FRP (Fiber Reinforced Polymer) reinforcement for concrete structures, Fédération Internationale du
25 Béton - fib, July, 130 pp.
- 26 16. Nanni, A., Di Ludovico, M. and Parretti, R., "*Shear strengthening of a PC bridge girder with NSM CFRP*
27 *rectangular bars*", Advances in Structural Engineering, Vol. 7, N° 4, 2004, pp.97-109.
- 28 17. CEB-FIP Model Code. Comite Euro-International du Beton, Bulletin d'Information n° 213/214, 1993.
- 29 18. EN 10 002-1, "*Metallic materials. Tensile testing. Part 1: Method of test (at ambient temperature)*", 1990,
30 35 pp.

- 1 19. ISO 527-5, "*Plastics - Determination of tensile properties - Part 5: Test conditions for unidirectional fibre-*
2 *reinforced plastic composites*", International Organization for Standardization, Genève, Switzerland, 1997, 9 pp.
- 3 20. Barros, J.A.O. and Sena-Cruz, J.M., "*Fracture energy of steel fibre reinforced concrete*", Journal of Mechanics
4 of Composite Materials and Structures, Vol. 8, N° 1, January-March, 2001, pp.29-45.
- 5 21. ACI Committee 318, 2002, "*Building code requirements for structural concrete and commentary*", American
6 Concrete Institute, Reported by ACI Committee 118.

7

8

TABLES AND FIGURES

- 1
- 2
- 3 **List of Tables:**
- 4 **Table 1** - Series of tests
- 5 **Table 2** - Properties of steel bars
- 6 **Table 3** - Main results
- 7 **Table 4** - Profitability index of the NSM technique
- 8 **Table 5** - Analytical vs experimental results (*ACI* and *fib* analytical formulations)
- 9 **Table 6** - Analytical vs experimental results for NSM technique
- 10 **Table 7** - Analytical vs experimental results of the contribution of the concrete and steel stirrups for the shear
- 11 resistance
- 12
- 13 **List of Figures:**
- 14 **Fig. 1** - Beam series
- 15 **Fig. 2** - Strengthening techniques: a) External Bonded, b) Near Surface Mounted
- 16 **Fig. 3** - Concept of $\delta_{p,K}$: deflection at $0.95F_{max,K}$ after $\delta_{Fmax,K}$
- 17 **Fig. 4** - Force vs deflection relations of the A10 beam series
- 18 **Fig. 5** - Force vs deflection relations of the A12 beam series
- 19 **Fig. 6** - Force vs deflection relations of the B10 beam series
- 20 **Fig. 7** - Force vs deflection relations of the B12 beam series
- 21 **Fig. 8** - Failure modes of A10 beam series
- 22 **Fig. 9** - Failure modes of A12 beam series
- 23 **Fig. 10** - Failure modes of B10 beam series
- 24 **Fig. 11** - Failure modes of B12 beam series
- 25 **Fig. 12** - Details of the failure modes: a) A12_M, b) B12_M, c) B12_IL, B10_IL and B12_VL, d) A10_VL
- 26 **Fig. 13** - Influence of the: a) CFRP shear reinforcement ratio, b) beam depth, c) longitudinal steel reinforcement
- 27 ratio, on the efficacy of the shear strengthening technique
- 28 **Fig. 14** - Representation of the profitability index for the NSM technique
- 29 **Fig. 15** - Data for the externally bonded shear strengthening technique

- 1 **Fig. 16** - Analytical vs experimental results (*ACI* and *fib* analytical formulation)
- 2 **Fig. 17** - Graphical representation of variables used in the formulation by Nanni *et al.* (for this example
- 3
$$\sum_i L_i = L_2 + L_3 + L_4$$
)
- 4 **Fig. 18** - Graphical representation of l_{max}
- 5 **Fig. 19** - Specimen of the pullout-bending tests
- 6 **Fig. 20** - Relationship between the contribution of the NSM CFRP shear strengthening system ($\Delta F_{max} = 2V_f$) and
- 7 the total effective length of this strengthening system ($L_{tot\ min}$)

1

Table 1 - Series of tests

Beam designation		Shear strengthening systems				
		Material	Quantity	Spacing (mm)	Angle (°)	
A Series	A10 Series	A10_C	-	-	-	-
		A10_S	Steel stirrups	6 ϕ 6 of two branches	300	90
		A10_M	Strips of S&P C-Sheet 530	8 \times 2 layers of 25 mm (U shape)	190	90
		A10_VL	S&P laminate strips of CFK 150/2000	16 CFRP laminates	200	90
		A10_IL	S&P laminate strips of CFK 150/2000	12 CFRP laminates	300	45
	A12 Series	A12_C	-	-	-	-
		A12_S	Steel stirrups	10 ϕ 6 of two branches	150	90
		A12_M	Strips of S&P C-Sheet 530	14 \times 2 layers of 25 mm (U shape)	95	90
		A12_VL	S&P laminate strips of CFK 150/2000	28 CFRP laminates	100	90
		A12_IL	S&P laminate strips of CFK 150/2000	24 CFRP laminates	150	45
B Series	B10 Series	B10_C	-	-	-	-
		B10_S	Steel stirrups	6 ϕ 6 of two branches	150	90
		B10_M	Strips of S&P C-Sheet 530	10 \times 2 layers of 25 mm (U shape)	80	90
		B10_VL	S&P laminate strips of CFK 150/2000	16 CFRP laminates	100	90
		B10_IL	S&P laminate strips of CFK 150/2000	12 CFRP laminates	150	45
	B12 Series	B12_C	-	-	-	-
		B12_S	Steel stirrups	10 ϕ 6 of two branches	75	90
		B12_M	Strips of S&P C-Sheet 530	16 \times 2 layers of 25 mm (U shape)	40	90
		B12_VL	S&P laminate strips of CFK 150/2000	28 CFRP laminates	50	90
		B12_IL	S&P laminate strips of CFK 150/2000	24 CFRP laminates	75	45

2

3

4

5

Table 2 - Properties of steel bars

Series	Stress	ϕ 6 (long.)	ϕ 6 (trans.)	ϕ 10 (long.)	ϕ 12 (long.)
A	f_{sym} *	622 MPa	540 MPa	464 MPa	574 MPa
	f_{sum} **	702 MPa	694 MPa	581 MPa	672 MPa
B	f_{sym} *	618 MPa	540 MPa	464 MPa	571 MPa
	f_{sum} **	691 MPa	694 MPa	581 MPa	673 MPa

* f_{sym} - Average value of the yield stress; ** f_{sum} - Average value of the maximum stress.

6

7

8

1
2

Table 3 - Main results

Beam designation	Shear reinforcing system	$F_{max,K}$ (kN)	$\frac{F_{max,K}}{F_{max,K_C}}$	$\frac{F_{max,K}}{F_{max,K_S}}$	$\delta_{p,K}$ (mm)	$\frac{\delta_{p,K}}{\delta_{p,K_C}}$	$\frac{\delta_{p,K}}{\delta_{p,K_S}}$
A10_C	-	100.40	1.00	0.59	2.80	1.00	0.17
A10_S	Steel stirrups	169.35	1.69	1.00	16.25	5.80	1.00
A10_M	Strips of sheet	122.06	1.22	0.72	3.75	1.34	0.23
A10_VL	Vertical laminates	158.64	1.58	0.94	12.86	4.59	0.79
A10_IL	Inclined laminates	157.90	1.57	0.93	30.96	11.06	1.91
A12_C	-	116.50	1.00	0.54	2.74	1.00	0.43
A12_S	Steel stirrups	215.04	1.85	1.00	6.34	2.31	1.00
A12_M	Strips of sheet	179.54	1.54	0.83	4.91	1.79	0.77
A12_VL	Vertical laminates	235.11	2.02	1.09	6.70	2.45	1.06
A12_IL	Inclined laminates	262.38	2.25	1.22	11.75	4.29	1.85
B10_C	-	74.02	1.00	0.61	2.00	1.00	0.23
B10_S	Steel stirrups	120.64	1.63	1.00	8.53	4.27	1.00
B10_M	Strips of sheet	111.14	1.50	0.92	4.40	2.20	0.52
B10_VL	Vertical laminates	131.22	1.77	1.09	6.83	3.42	0.80
B10_IL	Inclined laminates	120.44	1.63	1.00	4.27	2.14	0.50
B12_C	-	75.7	1.00	0.48	2.03	1.00	0.40
B12_S	Steel stirrups	159.1	2.10	1.00	5.09	2.51	1.00
B12_M	Strips of sheet	143.0	1.89	0.90	3.52	1.73	0.69
B12_VL	Vertical laminates	139.2	1.84	0.87	4.44	2.19	0.87
B12_IL	Inclined laminates	148.5	1.96	0.93	4.92	2.42	0.97

3

4

1

Table 4 - Profitability index of the NSM technique

Series		Beam designation	F_{max} (kN)	ΔF_{max} (kN)	l_{CFRP} (m)	$\Delta F_{max}/l_{CFRP}$ (kN/m)
A ($h = 0.30m$)	(4 ϕ 10)	A10_R	100.4	-	-	-
		A10_VL	158.64	58.24	4.8	12.13
		A10_IL	157.9	57.5	3.68	15.63
	(4 ϕ 12)	A12_R	116.5	-	-	-
		A12_VL	235.11	118.61	8.4	14.12
		A12_IL	262.38	145.88	7.35	19.85
B ($h = 0.15m$)	(4 ϕ 10)	B10_R	74.02	-	-	-
		B10_VL	131.22	57.2	2.4	23.83
		B10_IL	120.44	46.42	1.97	23.56
	(4 ϕ 12)	B12_R	75.7	-	-	-
		B12_VL	139.2	63.5	4.2	15.12
		B12_IL	148.5	72.8	3.91	18.62

2

3

4

Table 5 - Analytical vs experimental results (*ACI* and *fib* analytical formulations)

Beam designation	Experimental $V_f^{exp.}$ (kN)	ACI *		<i>fib</i> **		$V_f^{exp.}/V_{fd}^{ana}$ (ACI formulation)	$V_f^{exp.}/V_{fd}^{ana}$ (<i>fib</i> formulation)
		ε_{fe} (‰)	V_{fd}^{ana} (kN)	ε_{fe} (‰)	V_{fd}^{ana} (kN)		
A10_M	10.8	2.50	17.0	4.62	24.0	0.64	0.45
A12_M	31.5	2.50	33.8	3.75	38.9	0.93	0.81
B10_M	18.6	2.42	17.7	3.66	20.5	1.05	0.91
B12_M	33.7	2.42	35.0	2.79	30.9	0.96	1.09

5

* f'_c values were obtained at the age of the beam tests ($f'_c = 40.2$ MPa for A series and $f'_c = 46.5$ MPa for B series).

6

** f_{cm} values were obtained at the age of the tested beams.

7

8

9

10

11

1

Table 6 - Analytical vs experimental results for NSM technique

Beam designation	Experimental	Formulation by Nanni <i>et al.</i> ¹⁶			
		$\varepsilon_j = 4.0\text{‰}$, $\tau_b = 6.9 \text{ MPa}$ and $E_f = 166 \text{ GPa}$		$\varepsilon_j = 5.9\text{‰}$, $\tau_b = 16.1 \text{ MPa}$ and $E_f = 166 \text{ GPa}$	
	$V_f^{exp.}$ (kN)	V_{fd}^{ana} (kN)	$V_f^{exp.} / V_{fd}^{ana}$	V_{fd}^{ana} (kN)	$V_f^{exp.} / V_{fd}^{ana}$
A10_VL	29.1	10.9	2.67	19.8	1.47
A10_IL	28.8	13.4	2.15	19.8	1.45
A12_VL	59.3	23.9	2.48	39.6	1.50
A12_IL	72.9	33.6	2.17	55.4	1.32
B10_IL	23.2	7.4	3.14	17.3	1.34
B12_VL	31.8	10.5	3.03	19.8	1.61
B12_IL	36.4	18.8	1.94	35.6	1.02

2

3

4

Table 7 - Analytical vs experimental results of the contribution of the concrete and steel stirrups for the shear

5

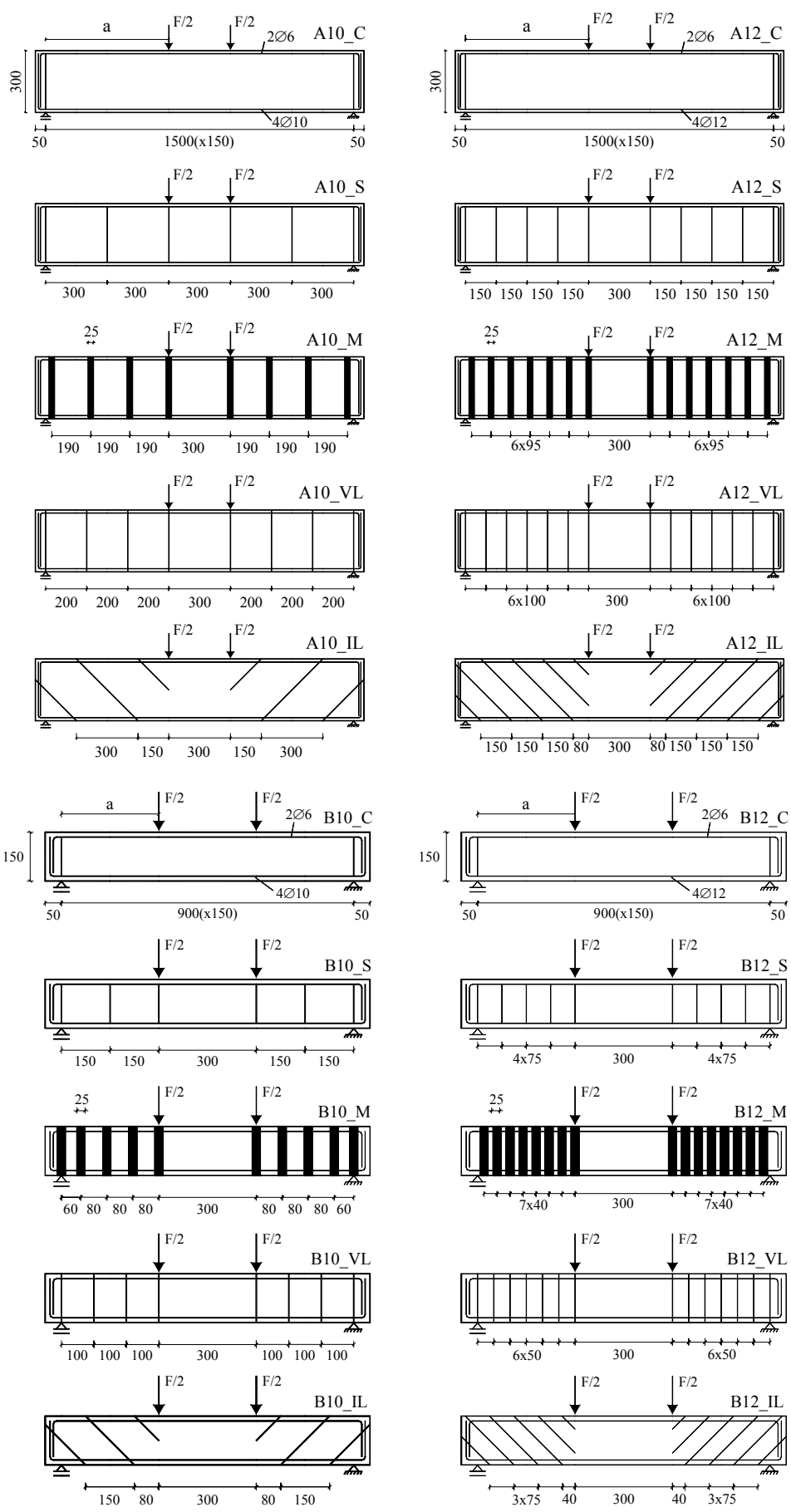
resistance

Beam designation	Experimental		Analytical (Portuguese Code)		$V_c^{exp.} / V_{cd}^{ana}$	$V_w^{exp.} / V_{wd}^{ana}$
	$V_c^{exp.}$ (kN)	$V_w^{exp.}$ (kN)	V_{cd}^{ana} * (kN)	V_{wd}^{ana} ** (kN)		
A10	50.2	-	34.9	-	1.44	-
A12	58.3	-	34.8	-	1.68	-
B10	37.0	-	18.6	-	1.99	-
B12	37.9	-	18.5	-	2.05	-
A10-S	50.2 ^{***}	34.5	-	21.8	-	1.58
A12-S	58.3 ^{***}	49.2	-	43.5	-	1.13
B10-S	37.0 ^{***}	23.3	-	19.7	-	1.18
B12-S	37.9 ^{***}	41.7	-	39.2	-	1.06

6

* $V_{cd}^{ana} = \tau_1 b_w d$; ** $V_{wd}^{ana} = 0.9 d \frac{A_{sw}}{s} f_{syd}$; *** Values that were obtained in the reference beams.

7



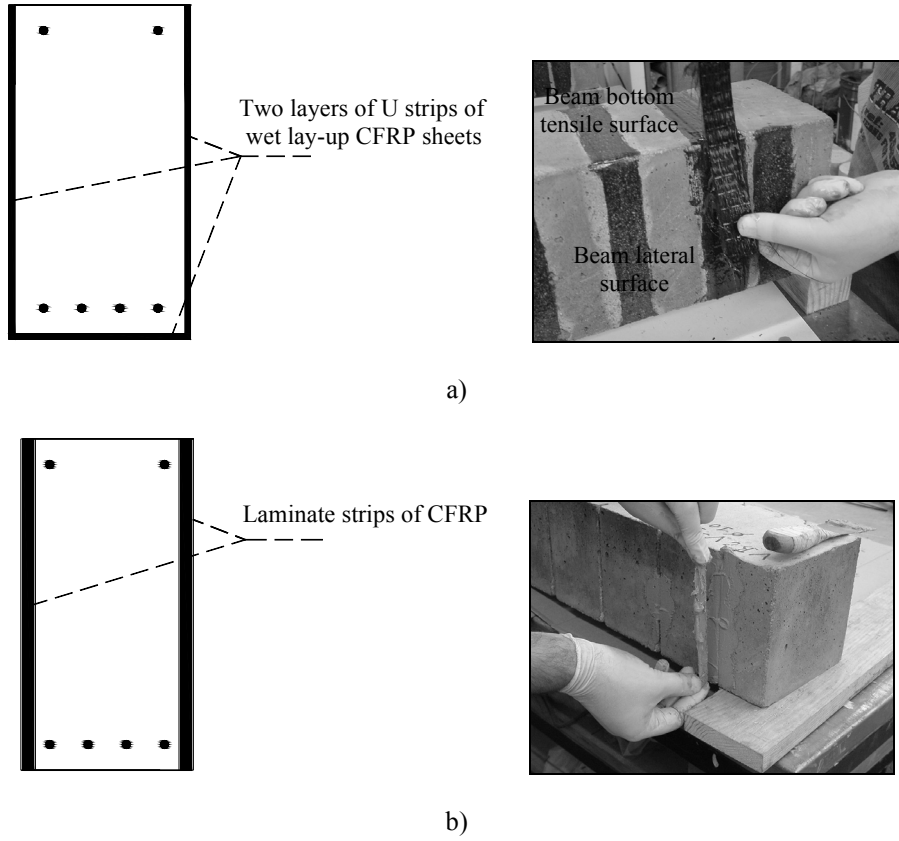
1

2

3

Fig. 1 - Beam series

1
2



3
4
5

Fig. 2 - Strengthening techniques: a) External Bonded, b) Near Surface Mounted

6
7
8
9

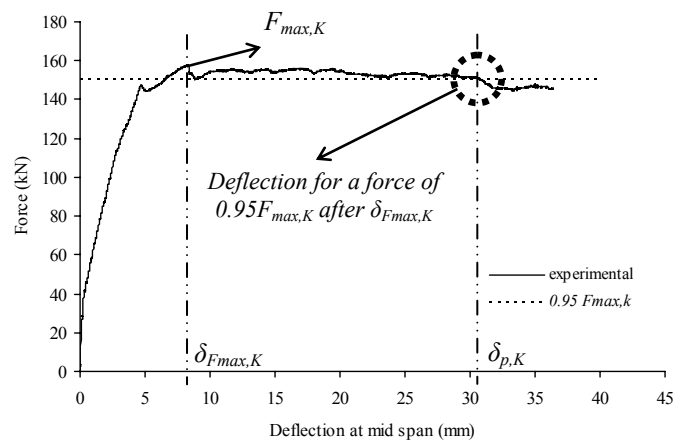


Fig. 3 - Concept of $\delta_{p,K}$: deflection at $0.95F_{max,K}$ after $\delta_{Fmax,K}$

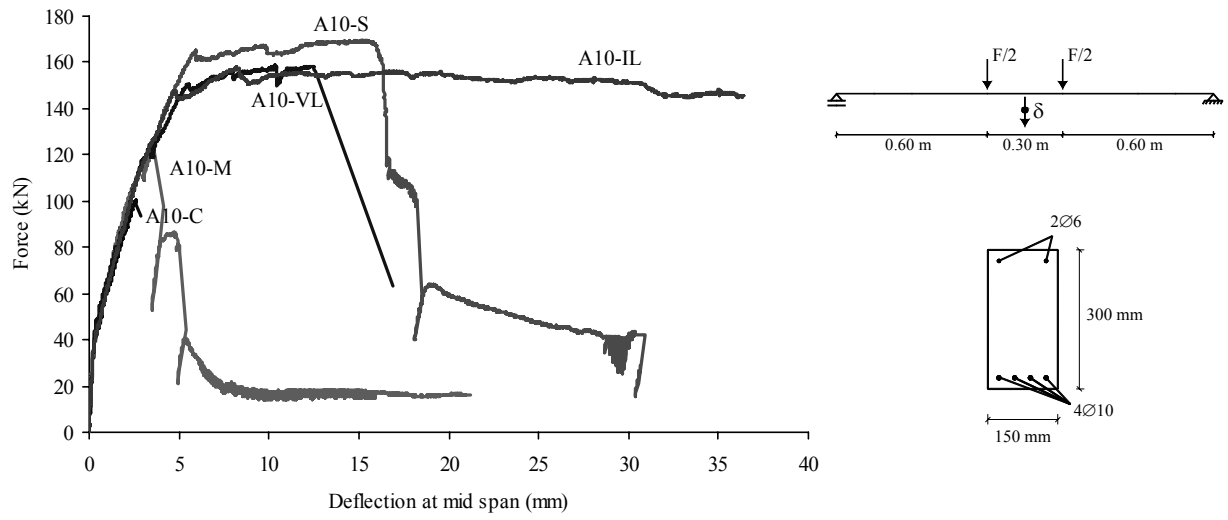


Fig. 4 - Force vs deflection relations of the A10 beam series

1
2
3

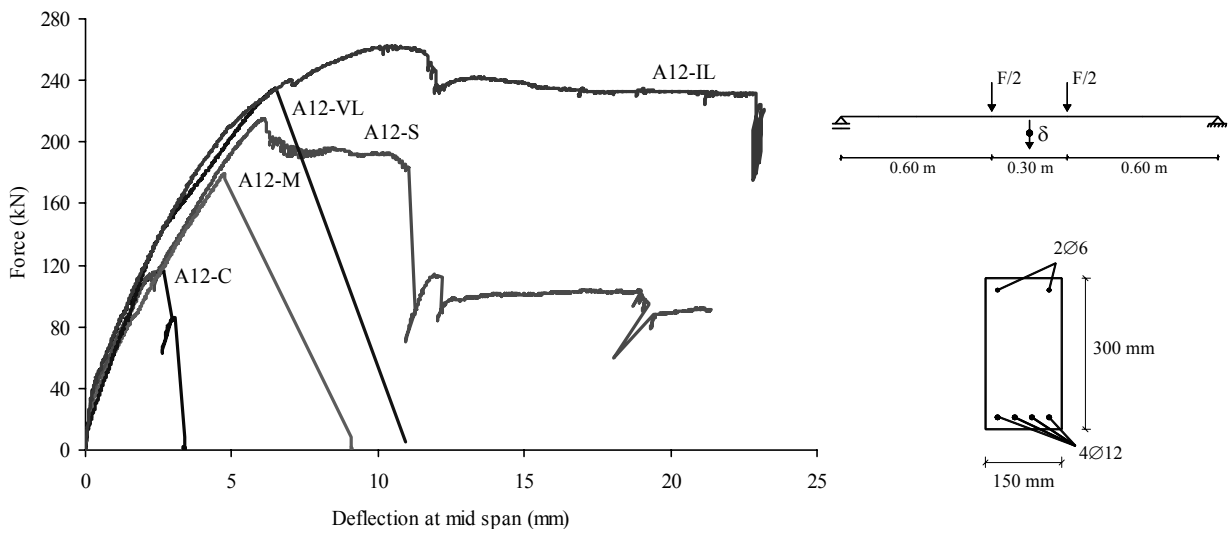


Fig. 5 - Force vs deflection relations of the A12 beam series

4
5
6
7
8
9
10
11
12

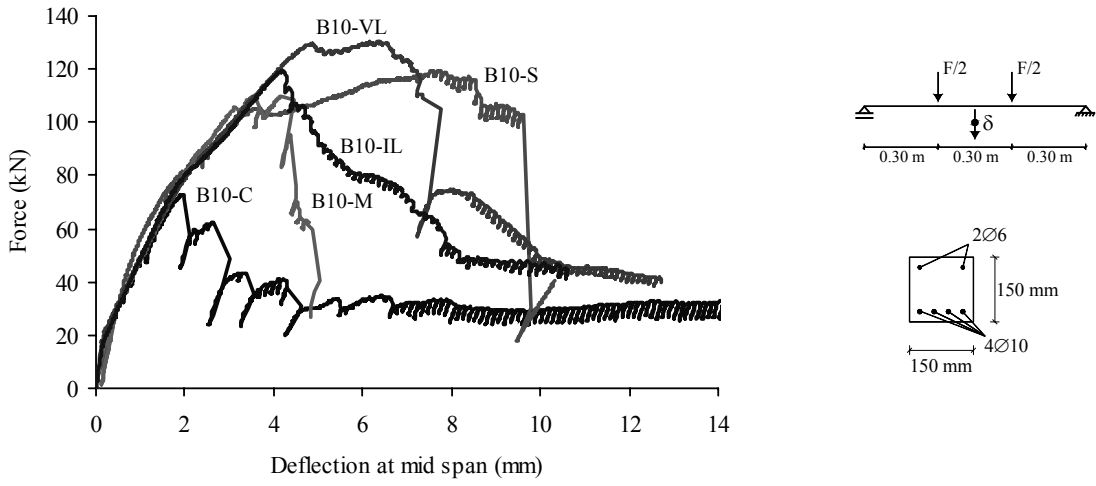


Fig. 6 - Force vs deflection relations of the B10 beam series

1
2
3

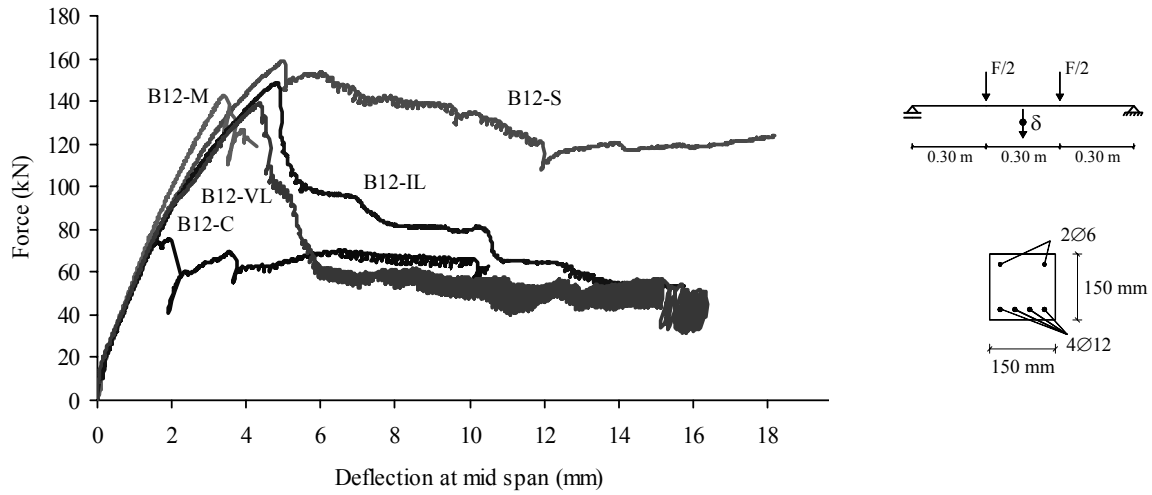
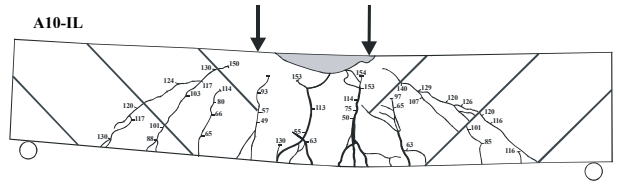
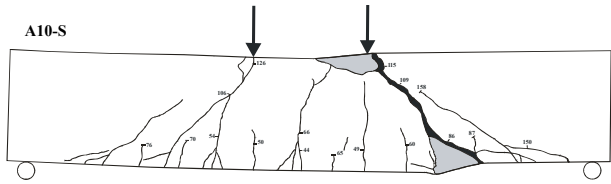
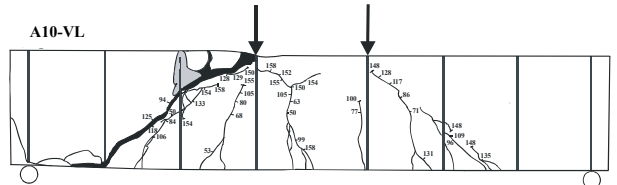
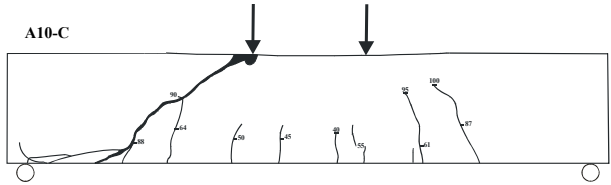
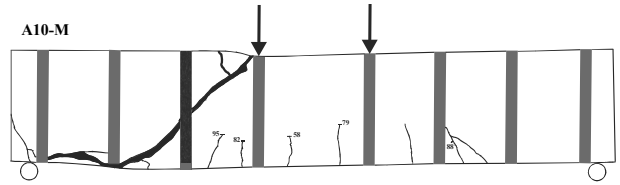
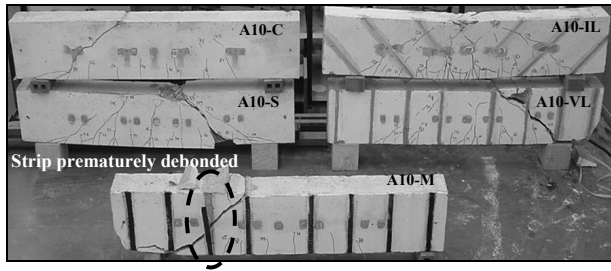


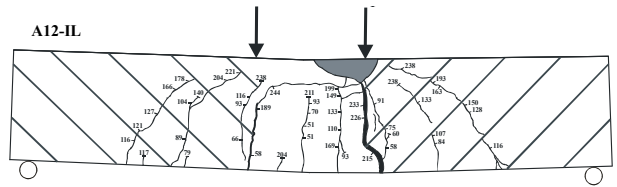
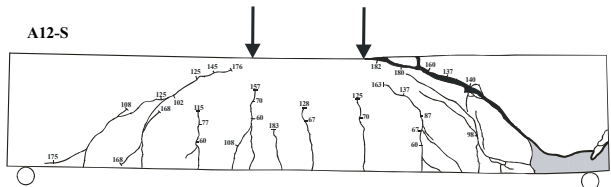
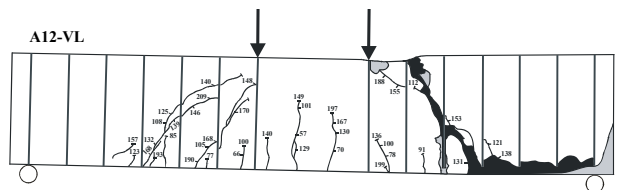
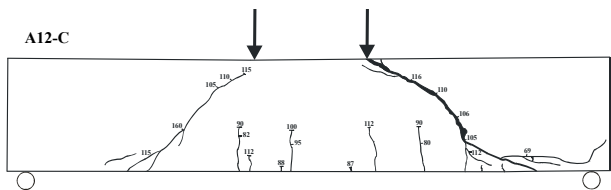
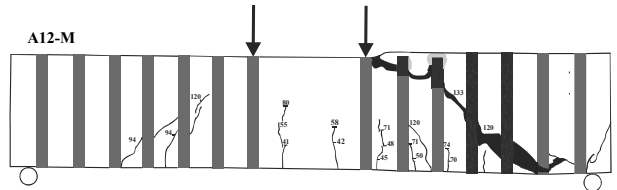
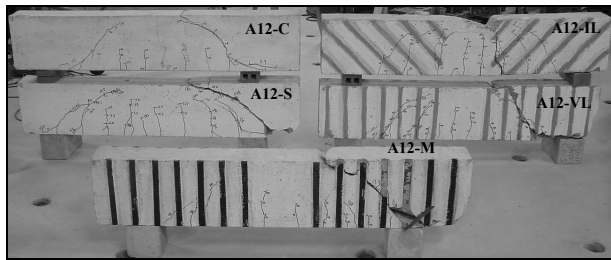
Fig. 7 - Force vs deflection relations of the B12 beam series

4
5
6
7
8
9
10
11



1
2
3

Fig. 8 - Failure modes of A10 beam series



4
5
6

Fig. 9 - Failure modes of A12 beam series

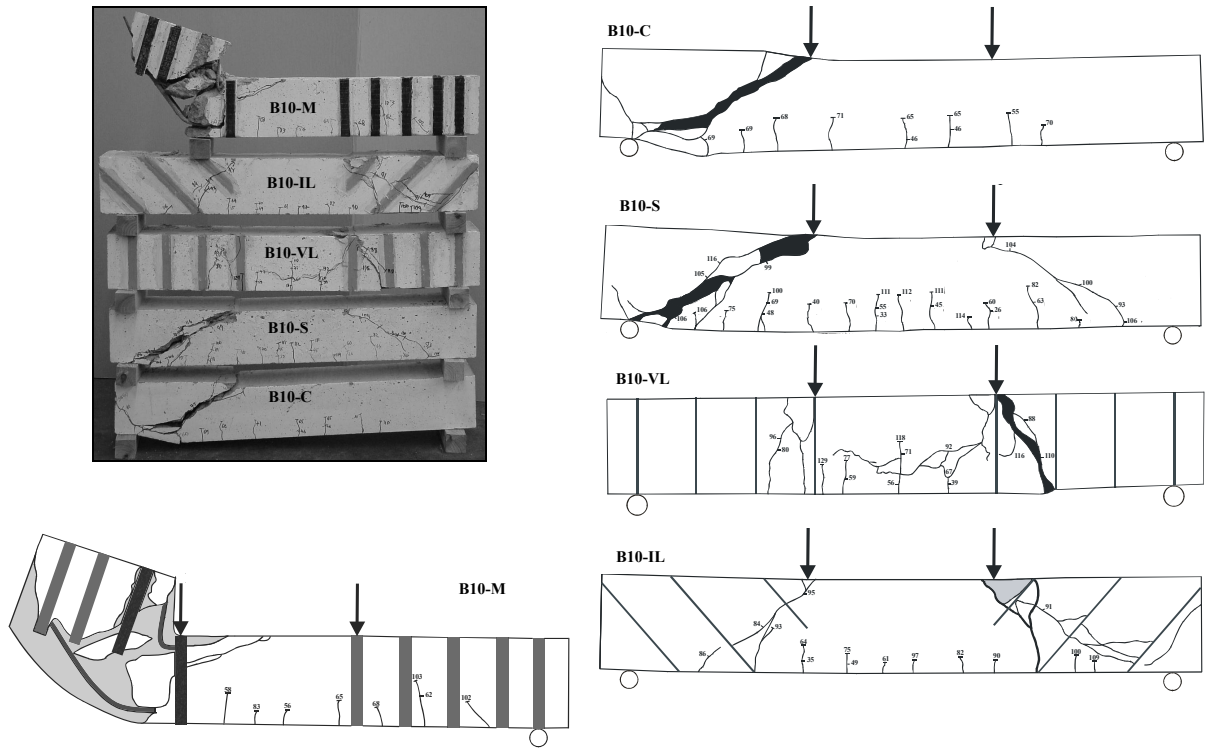


Fig. 10 - Failure modes of B10 beam series

1
2
3

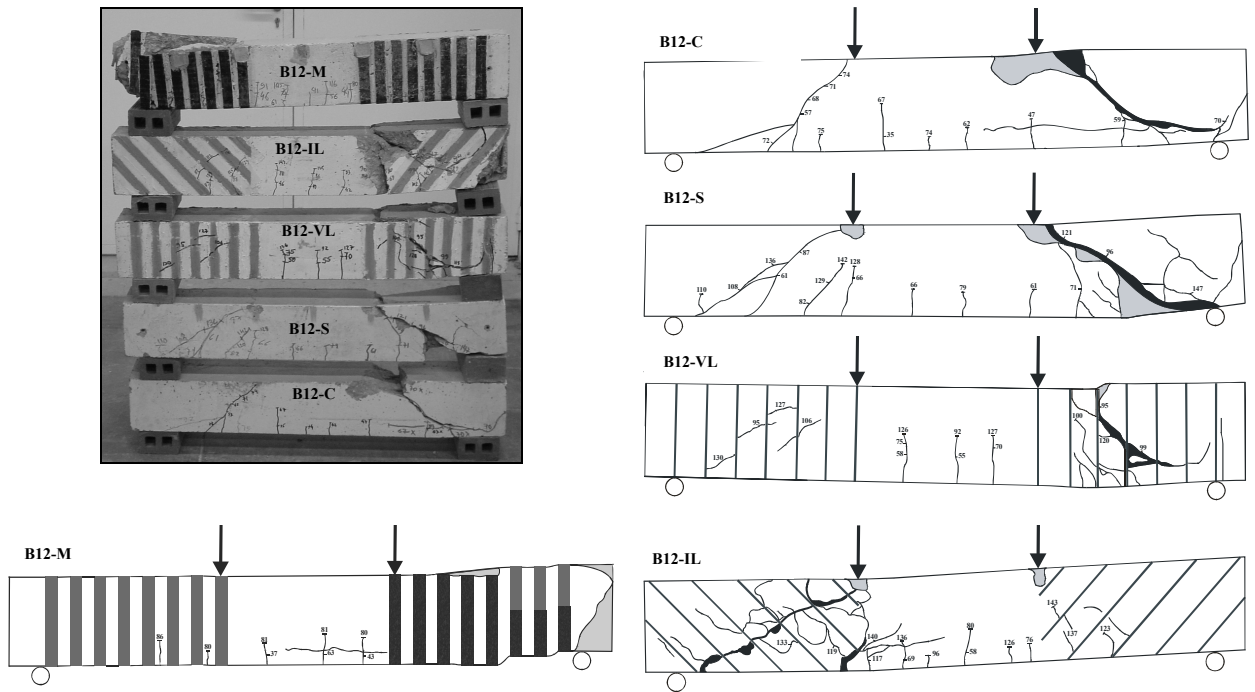
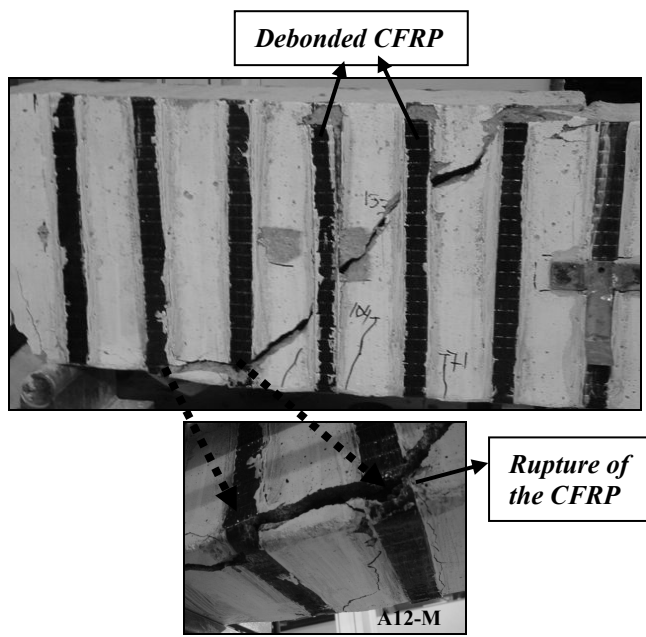


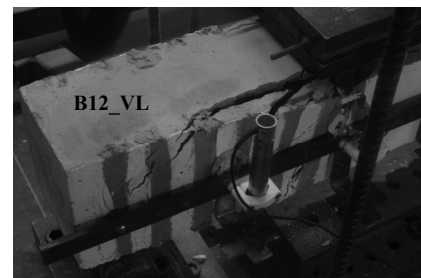
Fig. 11 - Failure modes of B12 beam series

4
5

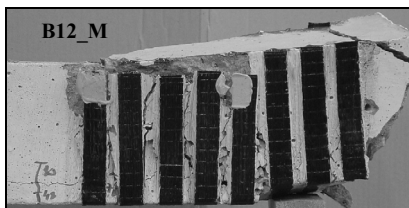
1



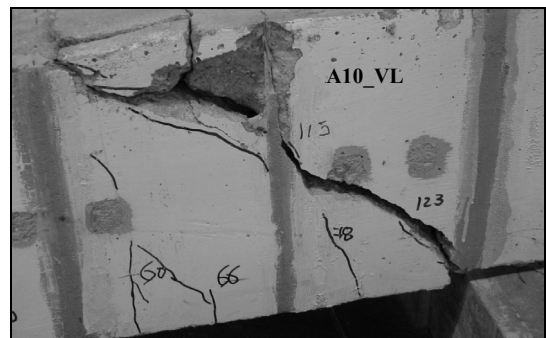
a)



c)



b)

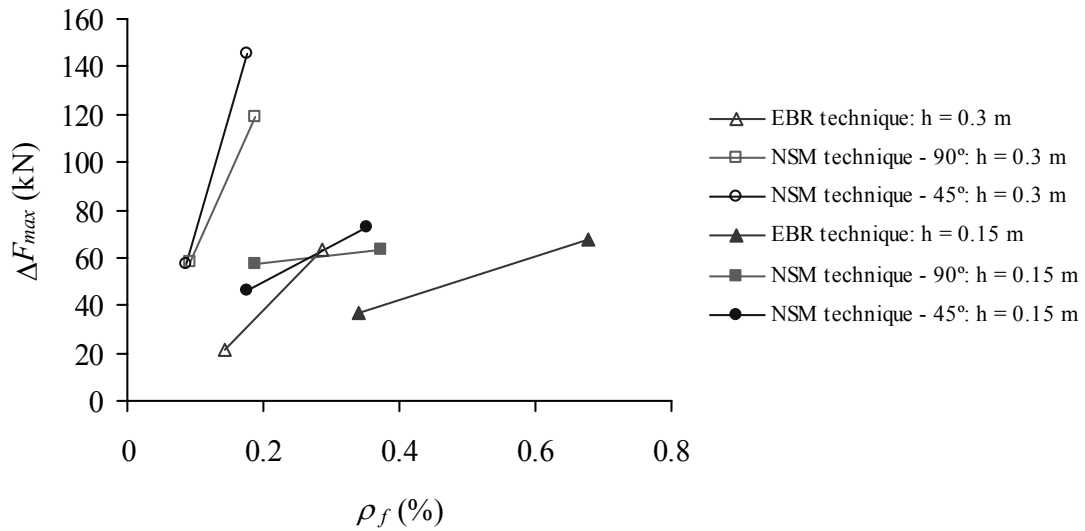


d)

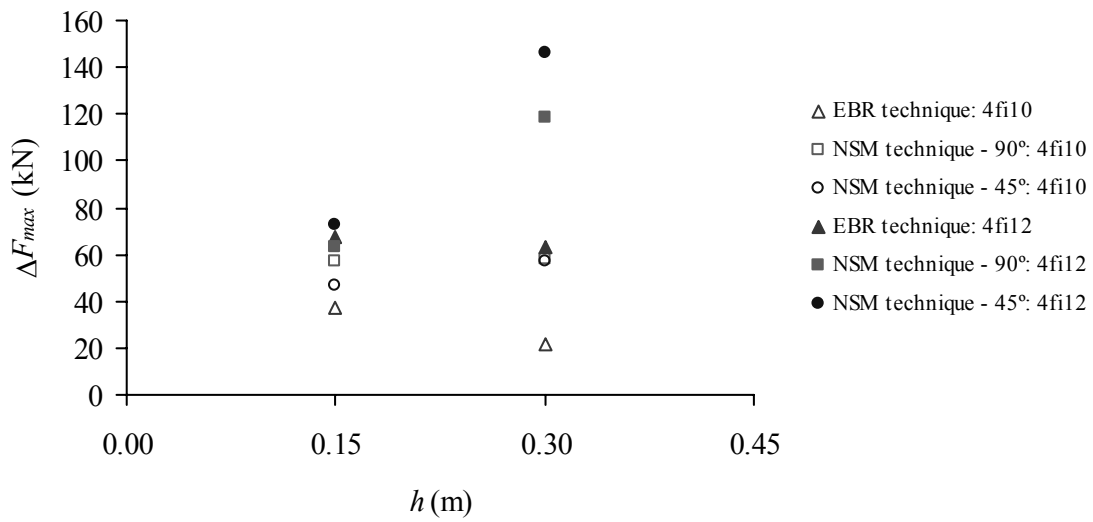
2 Fig. 12 - Details of the failure modes: a) A12_M, b) B12_M, c) B12_IL, B10_IL and B12_VL beams, d) A10_VL

3

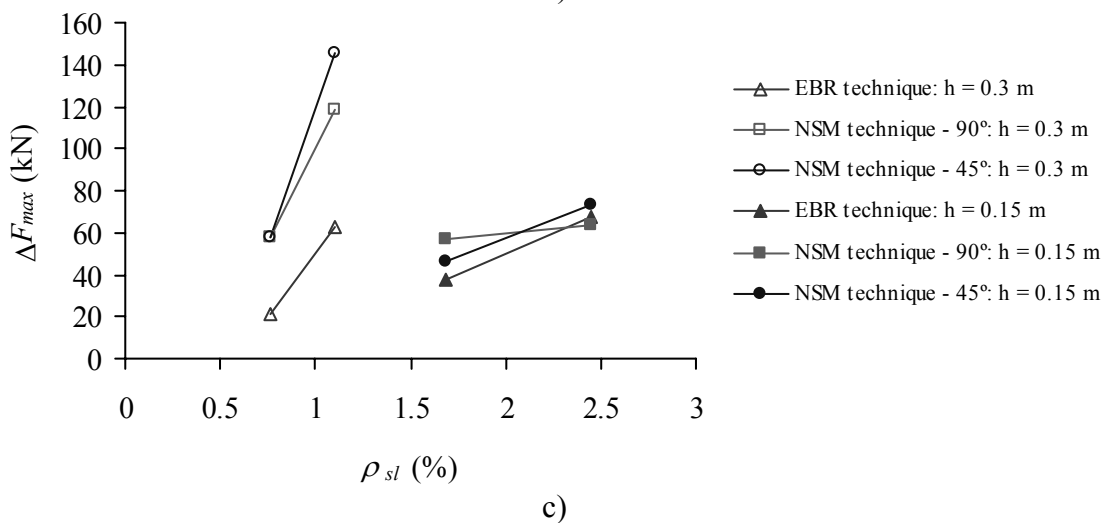
4



1
2
3



4
5



6
7

Fig. 13 - Influence of the: a) CFRP shear reinforcement ratio, b) beam depth, c) longitudinal steel reinforcement

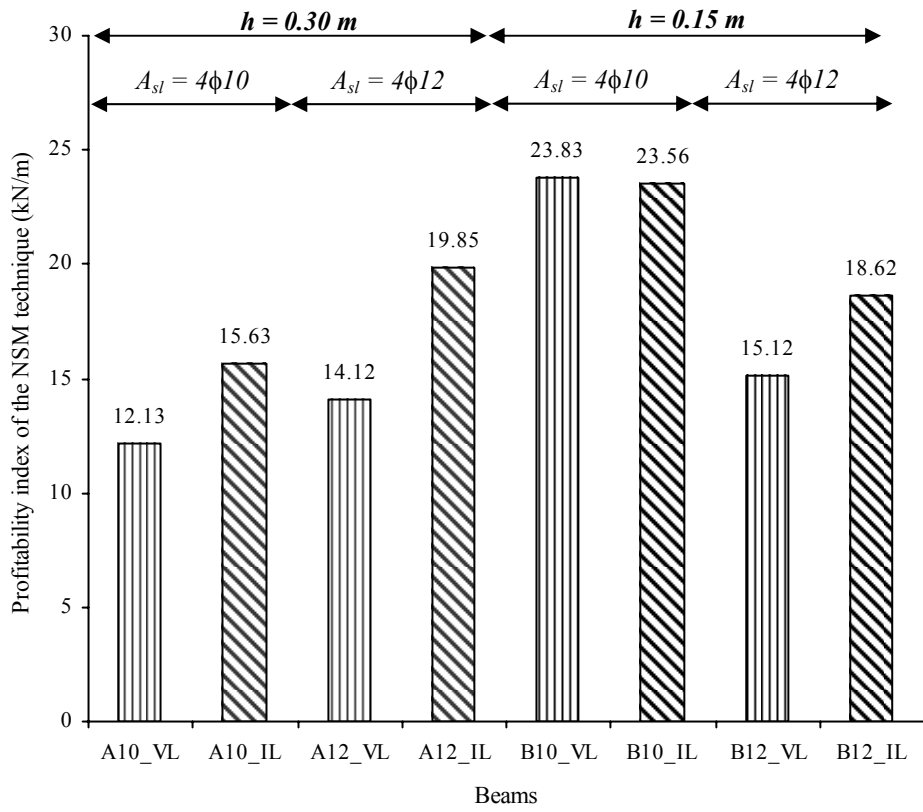
8

ratio, on the efficacy of the shear strengthening technique

9

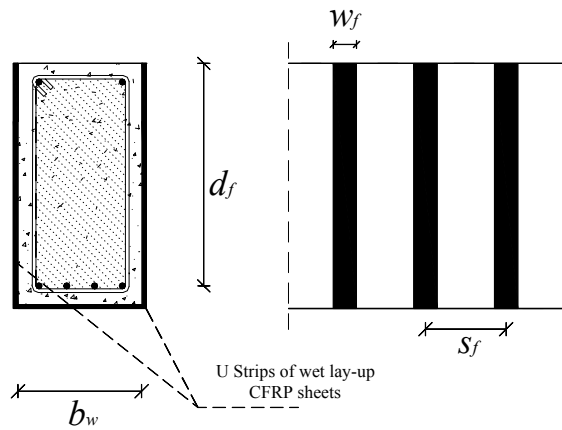
10

1
2
3



4
5
6
7
8

Fig. 14 - Representation of the profitability index for the NSM technique



9

Fig. 15 - Data for the externally bonded shear strengthening technique

10
11
12

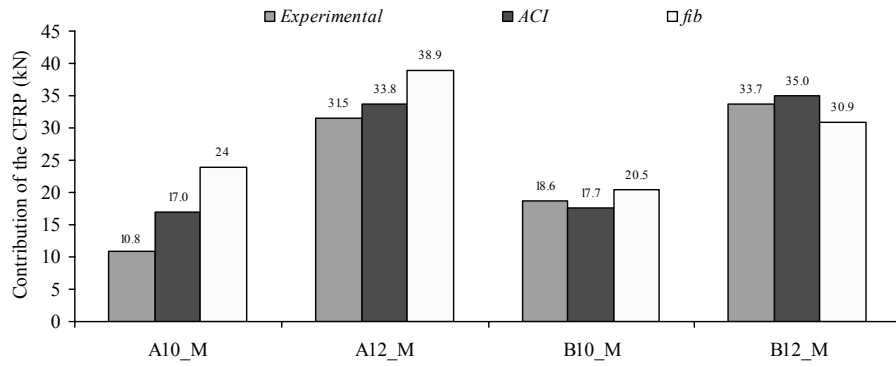


Fig. 16 - Analytical vs experimental results (*ACI* and *fib* analytical formulation)

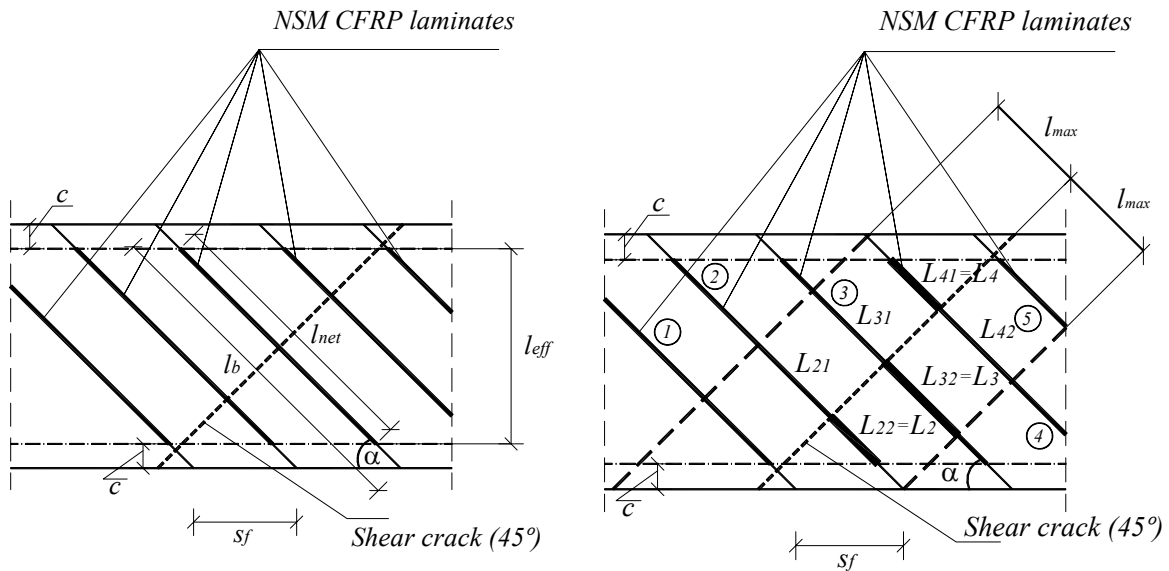


Fig. 17 - Graphical representation of variables used in the formulation by Nanni *et al.* (for this example

$$\sum_i L_i = L_2 + L_3 + L_4)$$

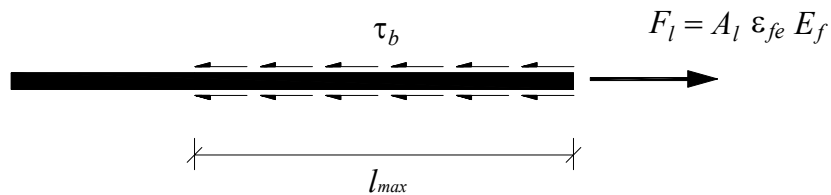


Fig. 18 - Graphical representation of l_{max}

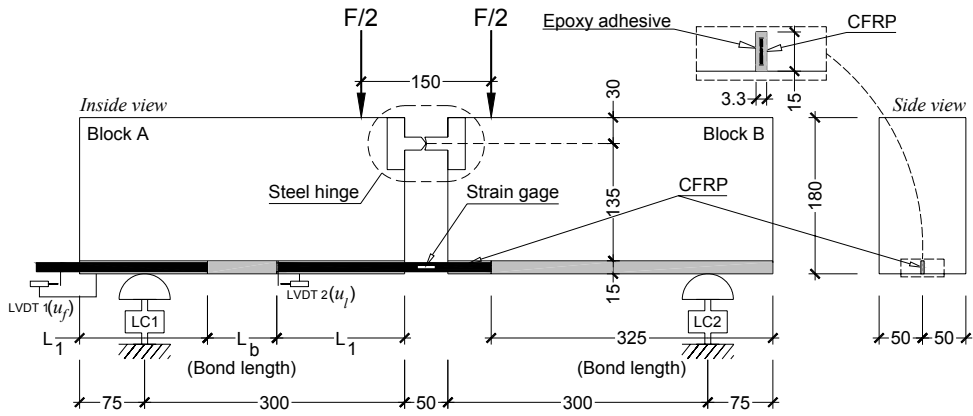


Fig. 19 - Specimen of the pullout-bending tests

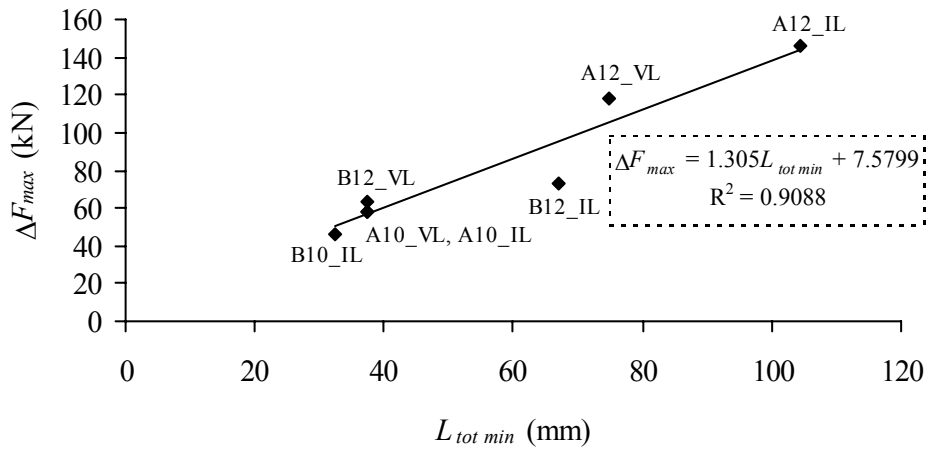


Fig. 20 - Relationship between the contribution of the NSM CFRP shear strengthening system ($\Delta F_{max} = 2V_f$) and the total effective length of this strengthening system ($L_{tot\ min}$)